

Design, synthesis, and evaluation of dioxane-based antiviral agents targeted against the Sindbis virus capsid protein

Ha Young Kim,^a Chinmay Patkar,^b Ranjit Warriar,^b
Richard Kuhn^b and Mark Cushman^{a,*}

^aDepartment of Medicinal Chemistry and Molecular Pharmacology, The Purdue Cancer Center,
School of Pharmacy and Pharmaceutical Sciences, Purdue University, West Lafayette, IN 47907, USA

^bDepartment of Biological Sciences, Lilly Hall, 915 West State Street, Purdue University, West Lafayette, IN 47907, USA

Received 22 February 2005; revised 27 April 2005; accepted 3 May 2005

Available online 31 May 2005

Abstract—Dioxane-based antiviral agents targeted to the hydrophobic binding pocket of Sindbis virus capsid protein were designed by computer graphics molecular modeling and synthesized. Virus production using SIN-IRES-Luc and capsid assembly were monitored to evaluate antiviral activity. A compound with a three-carbon linker chain connecting two dioxane moieties inhibited virus production by 50% at a concentration of 40 μ M, while (*R*)-hydroxymethyldioxane inhibited virus production by 50% at a concentration of 1 μ M. Both compounds were not cytotoxic in uninfected BHK cells at concentrations of 1 mM.

© 2005 Elsevier Ltd. All rights reserved.

The alphaviruses are pathogenic viruses with worldwide distribution. Infection can result in fever, rash, arthralgia or arthritis, lassitude, headache, and myalgia. There is presently no treatment available. The prototypic alphavirus is Sindbis virus, which is transmitted to humans through mosquito bites. It can be expected that the availability and study of new ligands for the hydrophobic binding pocket of Sindbis virus capsid protein will lead to a greater understanding of alphavirus capsid assembly and viral budding mechanisms. The present report documents the design and synthesis of a dioxane-based antiviral agent targeted against the Sindbis virus capsid protein.

The available crystallographic evidence supports the hypothesis that the intermolecular bonding of residues 108–111 in the N-terminal arm of the Sindbis virus capsid protein molecule to a hydrophobic pocket on an adjacent capsid protein molecule is involved in capsid assembly.¹ Furthermore, an apparent structural analogy between residues 108 and 111 in the N-terminal arm and residues 400 and 403 in the membrane E2 glycoprotein spikes suggests that the bonding of

these glycoprotein residues to the hydrophobic pocket of the capsid protein is involved in the budding of virus from the cell.¹ The proposed role of the capsid residues L108 and L110 in capsid assembly has been confirmed by mutational studies. Similarly, mutational studies of the E2 glycoprotein confirm that residues Y400 and L402 play critical roles in the budding process.^{1,2} These results indicate that small molecules that could bind to the hydrophobic binding pocket of the alphaviruses could effectively inhibit the viral replication cycle by blocking capsid assembly as well as budding from the cell. In fact, peptides centered around residues 397–403 of the E2 glycoprotein have been synthesized and have been found to be inhibitory for Sindbis virus budding.³

It is conceivable that the binding of the E2 glycoprotein spikes in the cell membrane to the hydrophobic pocket in the nucleocapsid protein results in a conformational change in the capsid that is conducive to budding. To investigate this hypothesis, an attempt was made to crystallize a nucleocapsid protein fragment 114–264 having an ‘empty’ hydrophobic pocket.⁴ However, the resulting X-ray structures of the crystalline Sindbis virus capsid proteins displayed a hydrophobic pocket occupied by one or two dioxane molecules derived from the crystallization solvent.⁴ The two dioxane molecules present in one of the protein structures occupy the same space as

Keywords: Antiviral; Sindbis virus capsid protein.

*Corresponding author. Tel.: +1 765 4941465; fax: +1 765 4946790;
e-mail: cushman@pharmacy.purdue.edu

the two leucine residues (108 and 110) present when the hydrophobic pocket is occupied by the N-terminal arm.

This result provided a template for drug design based on the structure of dioxane, and we have used it as a starting point for the design of potential antiviral agents containing two covalently linked dioxane moieties. The rationale for this proposal is that both dioxane moieties would have to dissociate simultaneously from the protein for the drug to dissociate, so the binding of the proposed ligand should be stronger than that of dioxane itself. Such a strategy circumvents the usual problems posed by peptide-based drug design, such as lack of peptide oral bioavailability resulting from metabolic instability and poor absorption.

Given this approach, our first task was to design a compound in which two dioxane molecules are linked using a linker chain of the appropriate length. Molecular modeling was performed using Sybyl[®] software and involved the removal of the capsid protein structure, except for a 10 Å sphere surrounding the dioxane molecules. The cut residues were blocked with free amino and carboxylic acid groups, and hydrogen atoms were added to the protein structure. The two dioxane molecules were extracted, linked, and then docked back into the empty pocket, and the energy was minimized using the MMFF94 force field while the protein structure was frozen. The structures of several ligands containing linker chains of various lengths were docked into the protein structure, leading to the realization that a three-carbon linker chain would allow the two dioxane moieties to occupy the same space as they do when they are not linked (Fig. 1).

The modeling result led us to select a three-carbon linker chain connecting two dioxane moieties as the first target compound **2**. Two additional ligands, **1** and **3**, were also designed in which one or two dioxane rings were attached to an aromatic substituent or a ketone functional group. The aromatic ring of compound **1** was incorporated to possibly stack with the indole ring of Try247. The carbonyl group of **3** could possibly act as a hydrogen bond acceptor and was included because it is readily available by hydrolysis of the intermediate dithiane **10** used to prepare **2**.

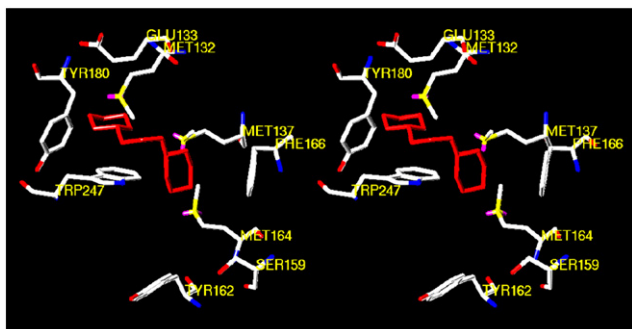
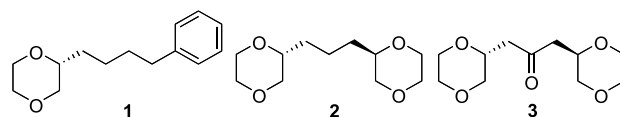


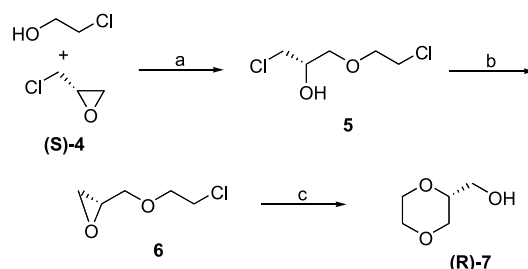
Figure 1. Molecular model of the binding of the dioxane dimer **2** in the hydrophobic binding pocket of Sindbis virus capsid protein. The figure is programmed for wall-eyed (relaxed) viewing.



These ligands are expected to block the interaction of the viral capsid protein with the N-terminal arm of an adjacent capsid protein molecule, which could inhibit capsid assembly. In addition, the occupation of the hydrophobic binding pocket could also be expected to block the binding of the viral capsid protein to the membrane-bound E2 glycoprotein spikes, thus inhibiting viral budding.

An efficient preparation of enantiomerically pure (*R*)-**7** is essential for the synthesis of the target compound **2**. Several research groups have prepared **7** in racemic form, or in an enantiomerically pure form, using a chiral resolving agent.^{5–8} So far, no group has reported an asymmetric synthesis, thus avoiding a chiral resolution of the racemate. In the present case, (*R*)-**7** was prepared in three steps from the commercially available epichlorohydrin (*S*)-**4** using several previously reported reactions (Scheme 1).^{5–8} The intermediates **5** and **6** were efficiently prepared in high yield by treatment of (*S*)-**4** with boron trifluoride diethyl etherate, followed by sodium hydroxide, and used in the next step without further purification. Intermediate **6** was then heated with sodium hydroxide at 90 °C for 2 h. The resulting product was obtained through a high-density continuous extraction with dichloromethane from a water layer, followed by purification by column chromatography to afford enantiomerically pure dioxane product (*R*)-**7**.

This well-optimized result allowed us to efficiently prepare a key intermediate (*R*)-**7** and to avoid a tedious resolution procedure. All physical properties and data, including ¹H and ¹³C NMR spectral data, were consistent with the literature values.⁷ The absolute configuration represented in structure (*R*)-**7** is consistent with the observed $[\alpha]_D^{20} -3.0$ (*c* 1, EtOH), which compares favorably with the $[\alpha]_D^{20} -6.06$ (*c* 2.5, EtOH) value reported in the literature for optically pure (*R*)-**7** prepared by a different route.⁷ The enantiomer (*S*)-**7** was also prepared from epichlorohydrin (*R*)-**4** by following the same reaction sequence, as shown in Scheme 1. As expected, (*R*)-

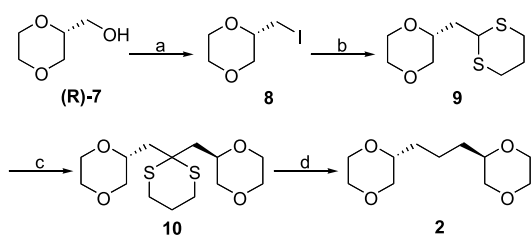


Scheme 1. Reagents and conditions: (a) $\text{BF}_3 \cdot \text{Et}_2\text{O}$, 45 °C, 1.5 h, 96%; (b) NaOH, water, rt, 2 h, 84%; (c) NaOH, water, 90 °C, 2 h, 36%.

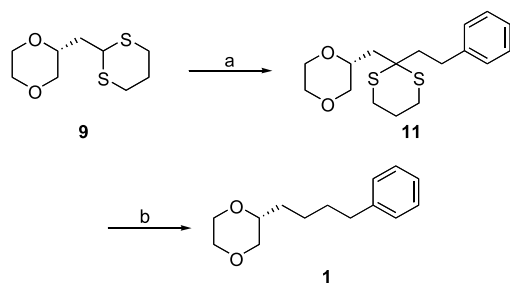
and (*S*)-**7** displayed optical rotations of opposite signs and equal absolute values.

(*R*)-**7** was converted to 2-iodomethyl-1,4-dioxane **8**^{9,10} with imidazole, triphenylphosphine, and iodine in a mixed solvent of toluene and tetrahydrofuran at ambient temperature.¹¹ Displacement of iodide from intermediate **8**^{9,10} with the lithium anion of 1,3-dithiane afforded the dithioacetal **9**, which was deprotonated with *n*-butyllithium and reacted with the iodide **8**^{9,10} in a mixed solvent of THF and HMPA to afford the penultimate intermediate **10**.^{12–14} Finally, the desired product **2**²⁰ was obtained through the desulfurization¹⁵ reaction with Raney nickel in refluxing ethanol (Scheme 2).

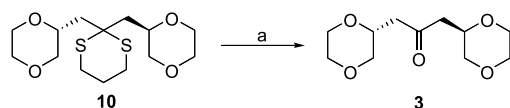
The first and second alkylation intermediates **9** and **10** were useful to provide additional target compounds **1** and **3** (Schemes 3 and 4). Deprotonation of intermediate **9** with *n*-butyllithium in THF–HMPA, followed by reaction of the anion with (2-iodoethyl)benzene, provided the product **11**. There was no *R_f* value difference between the product **11** and starting material **9** during TLC with an EtOAc–hexane solvent system. Column



Scheme 2. Reagents and conditions: (a) imidazole, PPh₃, I₂, toluene–THF, rt, 3 h, 93%; (b) 1,3-dithiane, *n*-BuLi, THF–HMPA 9:1, –70 °C to rt, 98%; (c) *n*-BuLi, **8**, THF–HMPA 9:1, –70 °C to rt, 76%; (d) Raney Ni, absolute ethanol, reflux, 5 h, 44%.



Scheme 3. Reagents and conditions: (a) *n*-BuLi, (2-iodoethyl)benzene, THF–HMPA 9:1, –70 °C to rt, 70%; (b) Raney Ni, absolute ethanol, reflux, 15 h, 71%.



Scheme 4. Reagents and conditions: (a) MeI, NaHCO₃, acetonitrile–water 1:1, 40 °C, 12 h, 80%.

chromatography failed to separate the remaining starting material from the product, only showing a mixture of **11** (70%) and **9** (30%) in the proton NMR. The mixture was used in the next reaction without further purification. The pure product **1**²⁰ was obtained from the Raney nickel desulfurization¹⁵ and purification by column chromatography (Scheme 3). The final transformation involved the hydrolysis^{12,16} of the dithiane **10** with excess methyl iodide and sodium bicarbonate in acetonitrile and water at 40 °C to yield the ketone product **3**²⁰ (Scheme 4).

Biological assays were focused on testing for inhibition of Sindbis virus production and for cytotoxicity in uninfected BHK cells. Two assays were employed to look for antiviral activity: virus production using SIN-IRES-Luc and in vitro core-like particle assembly. SIN-IRES-Luc is Sindbis virus with a firefly luciferase gene inserted at the 3' end of the genome, which is expressed off of an internal ribosomal entry site (IRES). The infectivity of the virus could be assayed directly as a measure of the luciferase amounts produced in infected cells over a period of time.

A cell viability assay was performed initially to plot a cytotoxicity curve for the compounds. A standard XTT-based colorimetric assay was employed, which involved treating BHK cells with various concentrations of the compounds and then using an XTT-conjugated substrate that formed an orange precipitate on reaction with mitochondrial dehydrogenases to determine cell viability. Spectrophotometric readings were taken at 450 nm and the intensity of the color was proportional to the viability of the cells. The cytotoxic concentrations were established by comparing the spectrophotometric readings for the treated and untreated cells. In the assay for the inhibition of Sindbis virus production, BHK cells were grown to confluency in 96-well plates. *Renilla* luciferase plasmid (Promega Corp.) was transfected into these cells. Expression of *Renilla* luciferase was used as an internal control to ensure that cellular transcription and translation were not affected by addition of the compounds. Four hours post-infection, cells were infected with SIN-IRES-Luc virus at a multiplicity of infection (MOI) of less than 1. Media containing the compounds at concentrations less than cytotoxic concentrations were added onto the infected cells, and the cells were further incubated at 37 °C for 12 h. Cell extracts were taken and luciferase assays were performed on the extracts using the LmaxII 96-well plate luminometer (Molecular Devices).^{17,18} The *Renilla* luciferase amounts were found to be equivalent in all the cells, untreated as well as treated with the compounds, thus indicating that the compounds had no detectable effect on the cellular transcriptional and translational machinery.

As judged by a reduction in firefly luciferase activity, compound **2** inhibited virus production with an EC₅₀ of 40 μM, which was not cytotoxic in uninfected BHK cells (Fig. 2). The concentration of **2** for 50% growth inhibition in uninfected BHK cells is greater than 1 mM (Table 1).

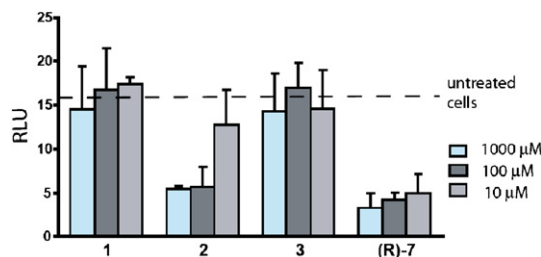


Figure 2. Inhibition of Sindbis virus (SIN-IRES-Luc) production.

Table 1. Antiviral activities and cytotoxicities of dioxane derivatives

Compound	EC50 (μM) ^a	CC50 (mM) ^b
1	>100	0.6
2	40	>1
3	>100	>1
(<i>R</i>)-7	1	>1

^aThe EC50 is the concentration of the compound resulting in a 50% reduction in virus production.

^bThe CC50 is the concentration of the compound causing a 50% growth inhibition of uninfected BHK cells.

Interestingly, the synthetic intermediate (*R*)-7 proved to be more potent than the target compound **2**, resulting in 50% inhibition of virus production at a concentration of 1 μM , which was not cytotoxic in uninfected cells (Table 1). This unexpected result led us to dock (*R*)-7 in the hydrophobic pocket of the Sindbis virus capsid protein by molecular modeling using the same procedure described for the dimer **2**, except that the amino group of Lys135 was allowed to rotate toward the primary hydroxyl group of one ligand molecules before the protein structure was frozen and the energy was minimized. The hypothetical structure displayed in Figure 3 indicates that it would be possible for the primary hydroxyl groups of two molecules of (*R*)-7 to hydrogen bond to the Lys135 side chain and the backbone carbonyl of Gly251. This model essentially maintains the orientations of the two dioxane molecules found in the crystal structure of Sindbis virus capsid protein. There are clearly other residues lining the binding pocket that would be capable of hydrogen bonding to different orientations of the ligand (*R*)-7, including Met132, Glu133, Met137, and Thr253. Two bound molecules of (*R*)-7 could also theoretically hydrogen bond to each other.

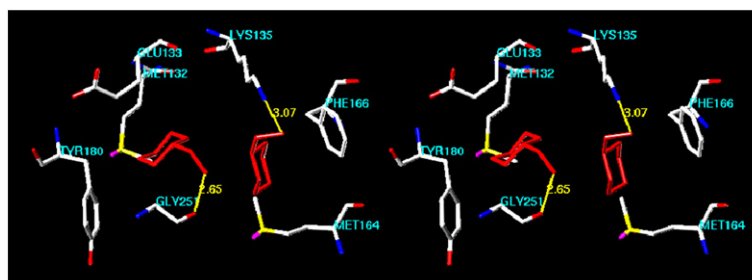


Figure 3. Molecular model of the binding of the dioxane derivative (*R*)-7 in the hydrophobic binding pocket of Sindbis virus capsid protein. The figure is programmed for wall-eyed (relaxed) viewing.

In the assembly assay, the alphavirus capsid protein was preincubated with each compound and then allowed to assemble with the addition of a synthetic 48-mer DNA oligonucleotide.¹⁹ We have previously carried out extensive studies and have shown that authentic nucleocapsid-like particles can be formed using purified capsid protein and nucleic acid.¹⁹ If arm-pocket binding is important in core-like particle assembly, the addition of the compound might be expected to inhibit the assembly process of the nucleocapsid. Core-like particles could be visualized either with ethidium bromide staining of the nucleic acid or with staining of the capsid protein with Coomassie blue. However, no inhibition was seen with any of the compounds when used at a tenfold molar excess over capsid protein.

In summary, several dioxane-based antiviral agents were rationally designed and synthesized based on the results prior to crystallographic studies of the Sindbis virus capsid protein. Computer graphics molecular modeling indicated that two solvent-derived dioxane molecules found the hydrophobic binding pocket during crystallography could theoretically be connected by a three-carbon linker without appreciable movement of the two dioxane rings. The linkage of the two dioxane moieties was expected to increase their affinity for the protein. The indicated compound **2** was synthesized and found to display a moderate antiviral effect, as judged by a 50% decrease in virus production (EC50) at a concentration of 40 μM . (*R*)-Hydroxymethyldioxane (**7**) displayed an EC50 of 1 μM . Both compounds were not cytotoxic in uninfected BHK cells at concentrations of 1 mM.

Acknowledgments

This work was made possible by the National Institutes of Health (NIH) through support with RCE Award U54 AI57153. This research was conducted in a facility constructed with support from Research Facilities Improvement Program Grant No. C06-14499 from the National Center for Research Resources of the National Institutes of Health.

References and notes

- Lee, S.; Owen, K. E.; Choi, H.-K.; Lee, H.; Lu, G.; Wengler, G.; Brown, D. T.; Rossmann, M. G.; Kuhn, R. J. *Structure* **1996**, *4*, 531.

2. Owen, K. E.; Kuhn, R. *J. Virology* **1997**, *230*, 187.
3. Collier, N. C.; Adams, S. P.; Weingarten, H.; Schlesinger, M. *J. Antiviral Chem. Chemother.* **1992**, *3*, 31.
4. Lee, S.; Kuhn, R. J.; Rossmann, M. G. *Proteins* **1998**, *33*, 311.
5. Younes, M. R.; Chaabouni, M. *Synth. Commun.* **1999**, *29*, 3939.
6. Tsivunin, V. S.; Zaripova, V. G.; Bikulova, V. Zh.; Zykova, V. V.; Kapustina, I. V. *J. Org. Chem. USSR* **1983**, *19*, 580.
7. Pallavicini, M.; Valoti, E.; Villa, L. *Enantiomer* **2001**, *6*, 267.
8. Wojtowicz, J. A.; Polak, R. J.; Zaslowsky, J. A. *J. Org. Chem.* **1971**, *36*, 2232.
9. Scholz, C. R.; Werner, L. H. *J. Am. Chem. Soc.* **1954**, *76*, 2701.
10. Evans, R. H.; Magee, J. W.; Schauble, J. H. *Synthesis* **1988**, 862.
11. Hosokawa, S.; Isobe, M. *J. Org. Chem.* **1999**, *64*, 37.
12. Nagumo, Y.; Oguri, H.; Shindo, Y.; Sasaki, S.; Oishi, T.; Hiramata, M.; Tomioka, Y.; Mizugaki, M.; Tsumuraya, T. *Bioorg. Med. Chem. Lett.* **2001**, *11*, 2037.
13. Matsuo, G.; Hori, N.; Nakata, T. *Tetrahedron Lett.* **1999**, *40*, 8859.
14. Andre, C.; Bolte, J.; Denuynck, C. *Tetrahedron: Asymmetry* **1998**, *9*, 1359.
15. Mehta, G.; Murthy, N. *J. Org. Chem.* **1987**, *52*, 2875.
16. Solladie, G.; Ziani-Cherif, C. *J. Org. Chem.* **1993**, *58*, 2181.
17. Schlesinger, M. J.; Cahill, D. *Virology* **1989**, *168*, 187.
18. Wachsman, M. B.; Damonte, E. B.; Coto, C. E.; Torres, R. A. *Antiviral Res.* **1987**, *8*, 1.
19. Tellinghuisen, T. L.; Hamburger, A. E.; Fisher, B. R.; Ostendorp, R.; Kuhn, R. J. *J. Virol.* **1999**, *73*, 5309.
20. Spectral data and optical rotations: (2*R*)-(4-Phenylbutyl)-[1,4]dioxane (**1**). ¹H NMR (CDCl₃) δ 7.57–7.40 (m, 5H), 4.05–3.74 (m, 6H), 3.52 (dd, *J* = 10.1 Hz, *J* = 10.1 Hz, 1H), 2.88 (t, *J* = 7.7 Hz, 2H), 1.96–1.55 (m, 6H); ¹³C NMR (CDCl₃) 142.5, 128.4, 128.3, 125.7, 75.3, 71.4, 66.8, 66.5, 35.8, 31.6, 31.5, 24.8; [α]_D²³ –1.4 (*c* 1, EtOH). 1,3-Bis-[(2*R*)-[1,4]dioxan-2-yl]propane (**2**). ¹H NMR (CDCl₃) δ 3.80–3.48 (m, 12H), 3.26 (dd, *J* = 10.0 Hz, *J* = 10.0 Hz, 2H), 1.54–1.26 (m, 6H); ¹³C NMR (CDCl₃) 75.3, 71.3, 66.8, 66.5, 31.6, 20.9; [α]_D²³ –0.2 (*c* 1, EtOH). 1,3-Bis-[(2*R*)-[1,4]dioxane-2-yl]-2-propanone (**3**). ¹H NMR (CDCl₃) δ 4.06 (m, 2H), 3.80–3.55 (m, 10H), 3.29 (dd, *J* = 10.0 Hz, *J* = 10.0 Hz, 2H), 2.63 (dd, *J* = 7.5 Hz, *J* = 7.5 Hz, 2H), 2.41 (dd, *J* = 5.1 Hz, *J* = 5.1 Hz, 2H); ¹³C NMR (CDCl₃) 205.4, 71.8, 71.0, 67.1, 66.7, 46.0; [α]_D²³ –0.1 (*c* 1, EtOH). (*R*)-2-Hydroxymethyl-[1,4] dioxane (*R*)-**7**. ¹H NMR (CDCl₃) δ 3.85–3.41 (m, 9H), 2.15 (br s, 1H); ¹³C NMR (CDCl₃) 75.5, 67.7, 66.2, 66.0, 61.9; [α]_D²⁰ –3.0 (*c* 1, EtOH).